Impact of noise and spatial constraints in Kuramoto oscillators

Author: Oriol Paricio Juan and Advisor: Dr Jordi Soriano Fradera
Departament de Física de la Matèria Condensada
Facultat de Física, Universitat de Barcelona, Diagonal 645, 08028 Barcelona, Spain.

Abstract: The Kuramoto model is one of the simplest models used to study collective synchronization. We consider the stochastic Kuramoto model with two sources of noise, *quenching* and *asymmetrical inducing*, in both a spatial independent (Erdős–Rényi) and a spatial dependent (random geometric graph) networks. We study how them affect to the order parameter and the critical coupling in the steady state. We observed that *quenched* noise mainly lowers the order parameter after synchronization, while the *asymmetrical inducing* noise causes an increase of critical coupling for synchronization to be achieved. Finally, we observed that both noise sources overall decreases synchronization capacity when a spatial dependence is introduced in the network.

I. INTRODUCTION

The whole is greater than the sum of its parts. This quote, attributed to Aristotle could be the simplest definition of both complexity and emergent phenomena. The concept of an emergent property is understood as a property that appears in macroscopic scales but not in microscopic ones, even though the macroscopic scale can be understood as the sum of plenty of microscopic systems [1].

One of most intriguing emergent properties is collective synchronization, understood as the spontaneous locking of a group of oscillators to one another in ensembles of them [2], a phenomenon that appears everywhere in nature, from the clapping in concerts [3] to flashing fireflies [4]. In our case, we are interested in the phenomenon from the point of view of neuronal population dynamics.

In 1967 the theoretical biologist A. Winfree published the first model to study collective synchronization [5]. This rather complex model was later simplified in 1975 by Y. Kuramoto, creating a model that can still be used to study several properties of this phenomenon, especially for systems where spontaneous synchronization happens [6].

The Kuramoto model is simple enough to be studied mathematically and simulated with most programming languages and, thus, is usually the model used as an example to explain this synchronization. Due to this fact this model is often described as *paradigmatic* [7].

When applying synchronization models to real world systems, the ideal Kuramoto model stops working due to fluctuations. Furthermore, these fluctuations are stochastic and do not add useful information to the problem under study. This character is commonly known as *noise* [8]. Noise has been regarded for decades as an 'annoying problem' when modeling systems, but it is a very important property in neuronal systems. It affects both the synaptic connections and the dynamics of the ion channels in the membrane [9] and therefore it is important for the dynamics of all neuronal networks.

Even though there exist plenty of types of noise and sources, the interaction between different noise contributions in a system has been barely studied. For instance, Sarkar *et al.* recently studied the interaction between *quenched* and *annealed* noises in Ref. [10]. Given the interest of the problem, and following some of the ideas introduced by Sarkar, here we explored the impact of two noise terms in the Kuramoto model, particularly when one of the noise terms increased asymmetries in the Kuramoto model.

II. METHODS

A. The Kuramoto model

The code used is a modification of the package `Kuramoto` obtained from Ref. [11], with the modification consisting in adding stochastic terns. Everything has been programmed in `Python 3.9`.

The simplest Kuramoto model consists of N coupled oscillators $\theta(t)$ with a natural frequency of ω. The evolution of the oscillators is governed by N first order differential equations:

$$\frac{d\theta_i}{dt} = \omega_i + \sum_{j=1}^{N} \frac{K_{i,j}}{N} sin(\theta_i - \theta_j), \tag{1}$$

where K is the coupling strength between two oscillators [6]. In our case we will study the model with a constant value of K. However, we will not consider that every oscillator is coupled with each other. As such, the equation can be rewritten as:

$$\frac{d\theta_i}{dt} = \omega_i + \frac{K}{M_i} \sum_{j=1}^{N} A_{i,j} sin(\theta_i - \theta_j), \tag{2}$$

where $A_{i,j}$ is 1 if i is coupled with j and 0 otherwise, and M_i is the number of oscillator coupled with the oscillator i. The initial phases for every oscillator take random values from a uniform distribution: $\theta_{0,i} \in [0, 2\pi]$. The natural frequencies have been chosen from a normal distribution $\omega_i \sim \mathcal{N}(0,\, 1)$.

Two sources of random noise are added to the phase

evolution equation:

$$\frac{d\theta_i}{dt} = \omega_i + \frac{K}{M_i}\sum_{j=1}^{N} A_{i,j} sin(\theta_i - \theta_j + \xi_{i,j}) + \eta_{i,j}, \quad (3)$$

where $\eta_{i,j}$ is a *quenched* noise and $\xi_{i,j}$ is an *asymmetrical inducing* noise.

The quenched noise η obeys:

$$\begin{aligned} \langle \eta_{i,j} \rangle &= 0, \\ \langle \eta_{i1,j1}\, \eta_{i2,j2} \rangle &= \sigma_\eta^2\, \delta_{i1,i2}\, \delta_{j1,j2}, \\ \eta_{i,j} &= \eta_{j,i}. \end{aligned} \quad (4)$$

And asymmetrical inducing noise ξ obeys:

$$\begin{aligned} \langle \xi_{i,j} \rangle &= 0, \\ \langle \xi_{i1,j1}\, \xi_{i2,j2} \rangle &= \sigma_\xi^2\, \delta_{i1,i2}\, \delta_{j1,j2}, \\ \xi_{i,j} &= \xi_{j,i}. \end{aligned} \quad (5)$$

Note that σ_η^2 and σ_ξ^2 are particularly important since they represent the strength of the noise.

In our study we do not consider the temporal evolution of the system. Instead, we will only study its steady state properties. Thus, to understand the effects of the two sources of noise on synchronization, there are two macroscopic descriptors that must be defined: r and K_c.

The quantity r is the module of the order parameter used to study the Kuramoto model, which is in general a complex variable described as:

$$z = r\, e^{i\psi} = N^{-1} \sum_{i=1}^{N} e^{i\theta}, \quad (6)$$

where ψ is the average phase of the angles. Thus, r is only the module and intuitively represents how similar are the phases. Indeed, $r = 1$ when all the oscillators are synchronized and 0 when none of them are [6].

The quantity K_c is related with the critical coupling, and represents the bifurcation point between a disordered and an ordered system. Even though there are plenty of analytical equations to estimate K_c [6, 12] none of them work well in a noisy formulation of the model. Thus, we chose the turning point on the growth of the order parameter in the steady state (see later in Fig. 1). Even though this is not a formal definition, it can be used to study the evolution of this parameter.

B. Networks generation

It is convenient to view the coupled oscillators as in a network, where nodes are each oscillator and links (or edges) are the coupling strength between oscillators. To investigate the impact of network structure, we have studied the Kuramoto model in two different network constructions. One of them without spatial constraints, i.e. purely topological, and one spatial–dependent. The latter is useful since better represents neuronal systems, which are embedded in a physical space.

For the purely topological network we considered the Erdős–Rényi (*random graph*) model, in which the probability of an edge being present is independent of the existence of the other ones. We have arbitrarily chosen a probability for the existence of a link between two nodes of $p = \frac{1}{2}$.

On the other hand, for the spatial model, we considered a *random geometric graph*, which is suited to include strong spatial constraints. As such, we have placed the oscillators in a dimensionless 1×1 space. There is also a probability of being a link between two nodes of $p = \frac{1}{2}$. However, the connection exists only if the distance between two nodes is $d \leq 0.3$. This distance has been chosen to be optimal for sake of the interest of the results after several explorations.

Note that for $d > \sqrt{2}$, both models would have been equivalent (d larger than spatial size). The code for the networks has been programmed with the help of the package `NetworkX 2.8.8`.

III. RESULTS

All the simulations have been made with 100 Kuramoto oscillators. For every value we have made a sweep of the coupling $K \in [0, 10]$ rad s^{-1}, in times in the range $t \in [0, 100]$ s with steps of 0.1 s. We have chosen this values due to limitations in computer processing power.

A. Erdős–Rényi network and noise

Firstly, we have made a few simulations in the Erdős–Rényi (ER) random graph model combining different noise strengths σ_η and σ_ξ.

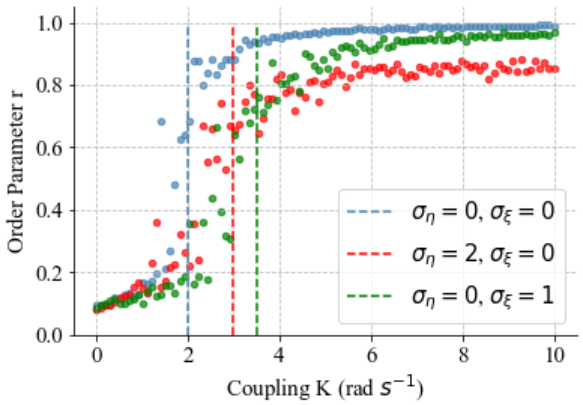

FIG. 1: Order parameter as a function of the coupling for 3 sets of noise strengths σ_η and σ_ξ, in a ER network. The critical coupling for each set is marked with vertical lines.

In Figure 1 we have plotted the average order parameter of the last 100 steps as a function of the coupling.

The position of the critical couplings has been chosen in the turning point, the position where the numerical derivative is 0. We observe that with a relatively small change in σ_ξ the critical coupling increases significantly. However, the decrease of the order parameter after the synchronization is only observable if we increase σ_η. It is also perceptible that the region where the synchronization is increasing is less stable to when we increase the value of σ_η so, in order to compute the value of K_c, we have carried out population averages.

To observe the interaction between the two sources of noise, we repeated simulations for different values of σ_η and σ_ξ and calculated r. The values for σ_ξ have a top value of 1 rad and the ones for σ_η a top value at 4 (see Table I). We note that an increase in σ_ξ substantially grows computation time, which is not so harsh for σ_η. For this reason, we have just taken a total of 25 values, and the intermediate ones were interpolated. This also helped to reduce computation power.

The same methodology was applied to explore the values of the critical coupling as a function of the noise terms (see Table II). In order to work with the exploration in this table, we had to work with the inverse of the critical coupling, K_c^{-1}, since it is possible for the system to never reach synchronization, which would provide $K_c \to \infty$ that can not be plotted. Additionally, although we do not have values of K_c for stronger noises, we know that they are typically bigger than 10, as indicated in the table.

In Figure 2 we show the results. We Note that in every phase diagram we have plotted $4\sigma_\xi$ and not σ_ξ due to limitations in the `matplotlib` package. In Figure 2(a) we observe that the value of the order parameter decreases while we increase any source of noise as far as σ_η is not zero. Moreover, up until the red frontier, we observe that r barely decreases when we increase σ_ξ. However, this could happen due to the smaller scale of σ_ξ. We see that the value is relatively close to 1 up until it harshly falls after reaching the red frontier. The values in the purple area have a lot of variability. As such the two values noted with (*) in Table I range from $r \sim 0.2$ to $r \sim 0.8$.

In Figure 2(b) we observe that the value of the critical coupling increases (i.e., lower K_c^{-1}) as we increase any source of noise. We can see that the critical coupling increases much faster while we increase σ_ξ. We note, again, the small range of this variable. Simulations made for values around the limit between the purple and the black areas show a bistability region around the critical coupling, quickly oscillating between complete and partial synchronization.

TABLE I: Values of the order parameter as a function of noise for the ER network averaged for 10 simulations.

$r \pm 0.01$		σ_η				
		0	**1**	**2**	**3**	**4**
σ_ξ (rad)	**0**	1.00	0.97	0.88	0.61(*)	0.20
	0.25	1.00	0.97	0.85	0.53(*)	0.18
	0.5	1.00	0.95	0.81	0.22	0.17
	0.75	1.00	0.92	0.75	0.20	0.15
	1	1.00	0.86	0.20	0.15	0.12

TABLE II: Values of the critical coupling as a function of noise for the ER network averaged for 10 simulations.

$K_c \pm 0.1(rad\,s^{-1})$		σ_η				
		0	**1**	**2**	**3**	**4**
$\sigma_\xi(rad)$	**0**	2.0	2.5	3.0	4.2	>10
	0.25	2.3	3.4	4.6	6.2	>10
	0.5	2.5	3.7	6.6	>10	>10
	0.75	3.0	4.0	9.3	>10	>10
	1	3.5	5.8	>10	>10	>10

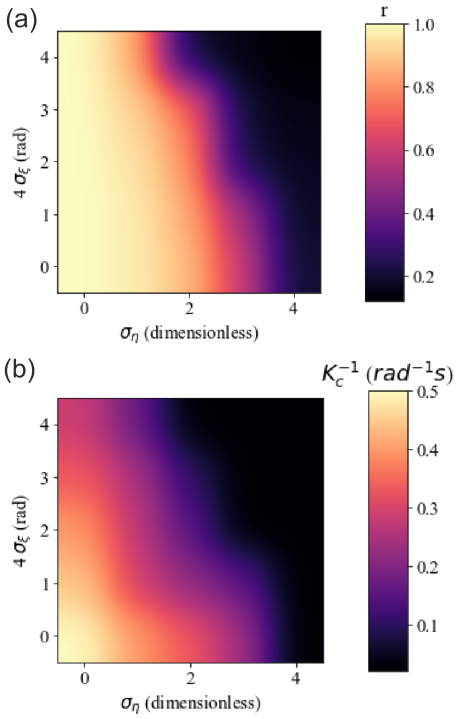

FIG. 2: Phase diagrams exploring the dependence of r or K_c as a function of the noise, and for the ER model. (a) For r. (b) For the inverse of K_c. The interpolation between values is Gaussian.

B. The random geometric graph model

Before fully introducing the impact of spatial embedding and noise terms, we found convenient to run a simple simulation comparing the ER and random geometric models without noise.

An example of a constructed random geometric graph is shown in Figure 3, which has a probability of having an edge between two nodes of $p = \frac{1}{2}$, and only when the

distance between two nodes is $d \leq 0.3$. We have chosen this distance arbitrarily. Note that if $d \geq \sqrt{2}$ we would get the same results that in the Erdős–Rényi model.

In Figure 5 we compare the two models, where we plotted the average order parameter of the last 100 steps as a function of the coupling. The position of the critical couplings has again been chosen in the turning point, the position where the numerical derivative is 0. From the plot it is clear that it is easier for the ER system to synchronize as compared to the random geometric, indicating that spatial constraints do affect network dynamics.

We next concentrated in the exploration of r and K_c for the geometric graph as a function of the noise. We also took 25 values and interpolated the intermediate ones.

For r, we consider now Table III. It shows that the order parameter decreases even with $\sigma_\eta = 0$. All the values (as compared to Table I) are also smaller. The value in $\sigma_\eta = 4$, $\sigma_\xi = 0.75$ rad is smaller than the one on

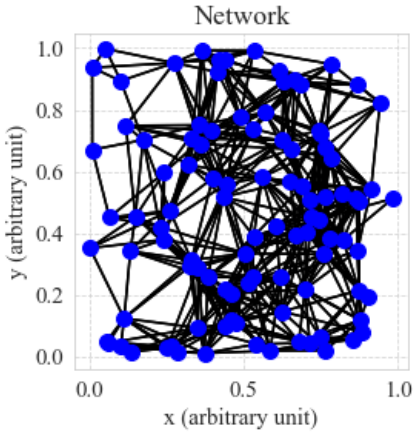

FIG. 3: Random geometric graph used for the simulations.

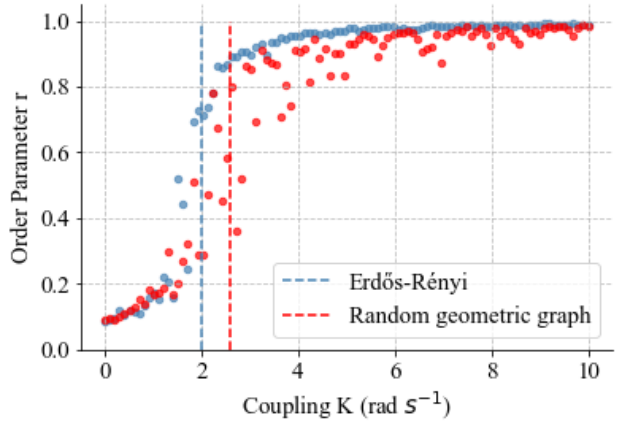

FIG. 4: Order parameter as a function of the coupling without noise in a Erdős–Rényi and in a Random geometric graph networks. The critical coupling for each data set is denoted by the vertical lines.

TABLE III: Values for the order parameter for the Random geometric graph network averaged for 10 simulations.

$r \pm 0.03$		σ_η				
		0	**1**	**2**	**3**	**4**
σ_ξ (rad)	**0**	1.00	0.97	0.11	0.09	0.08
	0.25	0.97	0.35	0.10	0.08	0.08
	0.5	0.94	0.20	0.09	0.07	0.06
	0.75	0.91	0.16	0.09	0.07	0.07
	1	0.81	0.11	0.07	0.06	0.05

$\sigma_\eta = 4$, $\sigma_\xi = 0.5$ rad. However, this is due the stochastic nature of the measures and both values mean complete disorder. No values in Table III have as much variability as the ones in the ER model, which were marked with (*).

TABLE IV: Values for the critical coupling for the random geometric graph network averaged for 10 simulations.

$K_c \pm 0.1 (rad\, s^{-1})$		σ_η				
		0	**1**	**2**	**3**	**4**
σ_ξ (rad)	**0**	2.6	5.8	>10	>10	>10
	0.25	3.3	>10	>10	>10	>10
	0.5	4.2	>10	>10	>10	>10
	0.75	6.7	>10	>10	>10	>10
	1	9.9	>10	>10	>10	>10

For the critical coupling, we can see in Table IV that, when spatial constraints are included, it is much more difficult for the system to synchronize. There are much more values for both σ that do not synchronize in our range of couplings. Again, for plotting those values we considered $K_c \to \infty$.

Overall, the qualitative behavior of r is shown in Fig. 5(a) is very similar to the one shown in Fig. 2(a), with a relatively stable order parameter near to 1 until it reaches the red boundary, followed by a harsh and fast decrease. However, as a major difference, the diagrams are shifted leftwards and downwards. This means that with weaker noise the synchronization stops being stable and the system does not reach synchronicity.

In Fig. 5(b) we observe that the value of the critical coupling K_c increases while we increase any source of noise, much more harshly here than before, though. The graph has a similar shape that in Fig. 2(b) but shrunk down. We Note that the plot shows the inverse of the critical coupling. Thus, this shrinking is translated into a really high growth of the critical coupling.

IV. DISCUSSION

One of the main limitations of this work is that every measure has been studied in its steady state. For further studies it would be interesting to study the dynamics of

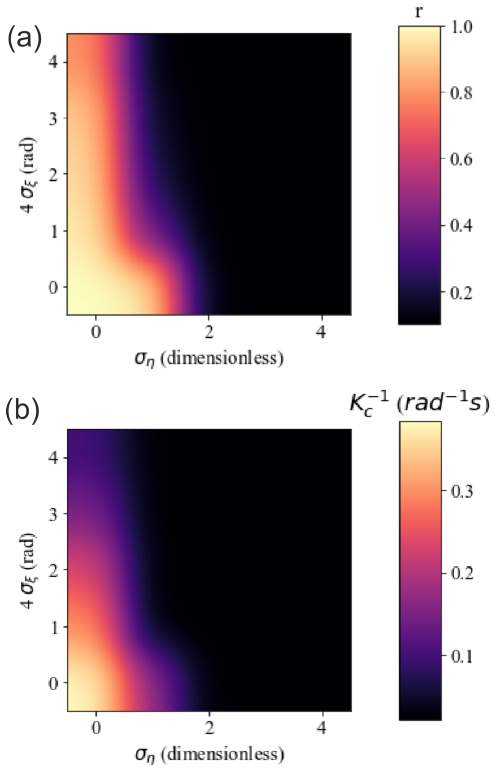

FIG. 5: Phase diagrams for the random geometric graph network. (a) Order parameter. (b) Inverse of critical coupling The interpolation is Gaussian.

the system along time and taking into account differences between network repetitions.

We note that the *asymmetrical inducing* noise ξ complicates synchronization. This can be observed analytically by analyzing Eq. (3), which can be written using trigonometric identities as:

$$\frac{d\theta_i}{dt} = \omega_i + \frac{K}{M_i}\sum_{j=1}^{N} A_{i,j}(sin(\theta_i - \theta_j)cos(\xi_{i,j}) + \\ + cos(\theta_i - \theta_j)sin(\xi_{i,j})) + \eta_{i,j}, \tag{7}$$

where the cosine term in a Kuramoto model is repulsive [13] and tries to desynchronize the system against the sine term.

The use of the random geometric graph is also interesting since it provides a step towards modeling living neuronal networks. In particular, this living networks often have nodes that aggregate (nodes closer to one another) as we can see in Figure 3 for $x \simeq 0.6$ and $y \simeq 0.5$. If aggregation is strong, synchronization would be highly local and the whole system could never synchronize.

V. CONCLUSIONS

We investigated synchronization in Kuramoto models and compared the behavior of an ER graph with one that included spatial constraints. In both cases, the system incorporated noise terms, and we explored their interplay.

We concluded that, firstly, the two noise terms included, *quenched* (η) and the *asymmetrical inducing* (ξ), acted differently. While η mainly reduced the order parameter in the steady state, ξ increased the critical coupling. Secondly, that the role of noises was essentially a faster decrease of both the order parameter and the critical coupling. And, thirdly, that that when networks with spatial constraints were considered, the effect of both noises was strengthened, meaning that spatial constraints made the system much more difficult to synchronize.

Acknowledgments

I would like to thank my advisor Dr. Jordi Soriano for his precious guidance through all this project and his wise advise. I would also like to thank my parents for keeping me motivated during this months and to my friends for being always there. Especially to Lídia for keeping me sane and to Jordi for his help with Python.

[1] P. W. Anderson, *Basic Notions Of Condensed Matter Physics*:20 (CRC Press,Cambridge 2019, 1st ed.).
[2] S. H. Strogatz, *Sync: The Emerging Science of Spontaneous Order* (Hyperion Press, New York 2003, 1st ed.).
[3] Z. Néda, E. Ravasz, Y. Brechet, T. Vicsek, and A.Ł. Barabási (2000), Self-organizing processes: The sound of many hands clapping, *Nature* 403, 849 .
[4] J. Buck and E. Buck (1976), Synchronous fireflies, *Science American* 234, 74.
[5] A. T. Winfree (1967), *Biological rhythms and behavior of populations of coupled oscillators*, *J. Theor. Biol.* 16, 15.
[6] Y. Kuramoto, *Chemical Oscillations, Waves and Turbulence* (Springer, New York 1984, 1st ed.).
[7] J. A. Acebrón, L. L. Bonilla, C. J. P. Vicente, F. Ritort, and R. Spigler (2005), The Kuramoto model, A simple paradigm for synchronization phenomena *Rev. Mod. Phys.*, 77(1):137.
[8] A. Destexhe, *Neuronal noise* (New York, Springer 2012, 1st ed.)
[9] A. A. Faisal et al. (2088), Noise in the Nervous System *Nat. Rev. Neurosci.* 9 (4): 292–303
[10] M. Sarkar (2020), " Noise-induced synchronization in the Kuramoto model on finite 2D lattice"
[11] F. Damicelli (2019). Python implementation Kuramoto (`https://github.com/fabridamicelli/kuramotos`)
[12] L. Q. English (2008). Synchronization of oscillators: an ideal introduction to phase transitions *Eur. J. Phys.* 29: 143
[13] P. Van Mieghem (2009). A complex variant of the Kuramoto model